

N74-14594

## DYNAMIC ANALYSIS OF A LONG SPAN, CABLE-STAYED FREEWAY BRIDGE USING NASTRAN

By W. L. Salus and R. E. Jones  
Boeing Aerospace Company

M. W. Ice  
Boeing Computer Services, Inc.

### SUMMARY

The dynamic analysis for earthquake- and wind-induced response of a long span, cable-stayed freeway bridge by NASTRAN in conjunction with post-processors is described. Details of the structural modeling, the input data generation, and numerical results are given. The influence of the dynamic analysis on the bridge design is traced from the project initiation to the development of a successful earthquake and wind resistant configuration.

### INTRODUCTION

During the summer of 1972, plans were formulated to design and build a new freeway bridge in Seattle, Washington, crossing the lower Duwamish waterway. This structure, called the West Seattle Freeway Bridge, is to provide a four lane highway and public transit connection between the city and the nearby residential and commercial area of West Seattle. The Duwamish waterway at this location is navigable by large vessels and the bridge is required to be both high and long, so as not to interfere with the water traffic. For these and esthetic reasons, a cable-stayed design was decided upon. Figure 1 illustrates the initial design concept<sup>(1)</sup>. Planview and elevation view curvatures are required by the orientations of the connecting freeway approach structures. The main foundation, supporting the tower from which the cables are suspended, is located near the edge of the waterway channel, and all foundations are supported by piles driven into the deep, soft, saturated soil at the site. The initial design incorporated a deck structure consisting of a slab supported by girders and a rigid-frame type of tower structure, as shown in the figure.

Because of Seattle's location in an earthquake zone, and because bridges such as the West Seattle design are subject to wind-induced oscillations, it was decided by the Seattle City Engineering Department to conduct a thorough dynamic analysis. The Boeing Company was engaged to perform this analysis.

(1) Configuration and detail design data shown in this paper were provided by the firm of Knoerle, Bender, Stone, and Associates, Inc., Consulting Engineers, Seattle, Washington; retained by the City of Seattle to perform the engineering design for the West Seattle Freeway Bridge project.

The initial work plan included analyses of a number of different bridge preliminary designs, including both concrete and steel deck constructions, in support of the development of a final structural design concept. Finite element analysis was decided upon. The need for parameter studies of the configurations of the deck, pile foundations, and the tower and pier structures was foreseen. Thus, a large number of analyses, with little setup time between them, was anticipated, and a simple computer model was desired. However, the nature of the deck design, particularly the combination of girders with a long span curved in both elevation and planform, suggested that a complex structural behavior might occur, requiring a correspondingly careful structural modeling. Therefore it was decided to perform two types of analyses, the first quick and simple, representing the deck structure as a single curved beam, and the second more detailed, representing the structural components of the deck by individual finite elements in the computer model. Figures 2 and 3 are computer plots which illustrate these two models. Though Figure 3 is quite crowded with element lines, the individual girder web and flange elements can be seen at the right end of the span. A verification of the validity of the data computed with the simple model was planned to be obtained by a comparison of its modes and frequencies with those of the complex mode. This, in addition to arranging the computer coding to facilitate convenience in parameter studies, constituted the overall work plan for the structural modeling.

The specific goals of the dynamic analysis were the calculation of earthquake-induced stresses in the structure and the calculation of the critical windspeeds at which aerodynamically induced unstable deck oscillations could occur. Predictions of these data were made on the sequence of bridge designs which were generated as the project developed. It was found that both earthquake- and wind-induced responses are critical design conditions, and that the initial types of design configurations were not capable of withstanding these responses (Reference 1). On the basis of these early evaluations, criteria were developed for achieving dynamically satisfactory designs. Principally, these criteria specified the frequencies of the structural vibration modes to avoid large earthquake response and specified the deck torsional stiffness and the shape of the deck cross-section to avoid wind-induced unstable oscillations.

The criteria led to a modification of the deck cross-section to the slant-sided, multi-cell closed section shown in Figure 4a and to a modification of the tower to the wall-type configuration shown in Figure 4b. Designs incorporating the features of Figure 4 are satisfactory for both wind- and earthquake-induced dynamic response. Currently, additional studies are underway to optimize this basic design for earthquake resistance by adjusting its vibration mode frequencies to avoid the known frequencies of principal earthquake excitation. This work has achieved a significant reduction in the required reinforcing steel. The detail design phase of the work will continue to be supported by dynamic analysis until the design is finalized, in the fall of 1973.

This paper discusses those aspects of the work which are associated with the finite element idealization and the modal analysis. This work has been done with the NASTRAN system, which has proved to be a highly effective tool in this application.

## SELECTION OF NASTRAN

The NASTRAN system has several features which are advantageous for this problem, leading to its choice over other available structural analyzers. Several of these features are mentioned briefly in this section; others are discussed in more detail in later descriptions of the finite element idealizations. The use of combined cylindrical and cartesian coordinates was helpful in modeling the combined circular arc and straight line geometry of the bridge planform. The ability to specify nonstructural mass on the CBAR elements was useful since structural data were provided in the form of mass per running foot on major structural members. The multi-point constraint feature was particularly useful for representing the connectivity between different portions of the bridge structure. In particular, this was necessary to represent proper connections of the deck structure to the supporting cables, piers, and the tower, and to represent the footing connections to the piles. Multipoint constraints were also used in the more complex model (called the 3D model) to connect the individual girders to the deck slab. The NASTRAN plotting feature was used to obtain pictorial descriptions of the structural vibration modes. In the case of seismic analysis this is particularly important, because seismic response is strongly dependent on both the shape and the direction of principal modal motions. Hence, pictorial data permit a quick, qualitative assessment of the likely seismic importance of the structural modes. And finally, since the seismic and flutter analyses were done by additional processing of the results of the modal analysis, a convenient data access system such as the NASTRAN checkpoint/restart tape feature was required. Thus NASTRAN appeared to be particularly well suited to the technical requirements of the problem.

Additional motivation for using NASTRAN was provided by the availability of Boeing's input language, SAIL, which has been adapted for NASTRAN input. Most of the bulk data were generated automatically by the use of SAIL. Bridge geometric data were provided in equation form, which can be coded directly in SAIL's automatic grid point generation format. In addition, SAIL has the capability to generate data within special (parameter-controlled) subroutines, called external data generators. External data generators were used to generate NASTRAN multi-point constraint equations, the girder plus slab deck simulation of the 3D model, and the pile foundation simulations. These data generation routines are designed such that a set of input parameters controls the generation of data. By changing a few of these parameters, a complete new set of data can be produced, simulating a new design concept. Through such automatic input generation it was possible to obtain rapid turnaround of analyses to support the design development.

A separate computer program was written to perform the seismic analysis, using the response spectrum analysis method. This analysis requires the mode shapes, frequencies, generalized mass, and internal element forces produced in the modal analysis. The NASTRAN checkpoint/restart tape provided access to these data. Since NASTRAN normally does not checkpoint element forces, a simple Alter was used to checkpoint the element force file OEF1.

## REPRODUCIBILITY OF THE ORIGINAL PAGE IS POOR.

### BEAM (STICK) FINITE ELEMENT MODEL

#### Purpose

To perform dynamic analysis in support of design trade studies, a simple model of the bridge structure, easily modified and with reasonably short run time, was set up. Called the "stick" model, it uses simple, beam type representations of all structural components. Because of the simplicity of this model, it was possible to make parametric studies of important parameters, such as the tower stiffness and the earth lateral resistance to pile motions, in order to assess the importance of these factors early in the program.

#### Description of the Model

There were two basic configurations from which the parameter studies were made: the steel bridge alternate and the concrete bridge alternate. The models of each of these configurations included the tower, piers (four piers in the steel model, three in the concrete model), the footings, piling, and earth springs to represent lateral earth resistance to pile motions, and the deck itself. The modeling of the piers, footings, piles and earth springs was of primary importance in seismic response. The deck modes and consequently the deck modeling were of primary interest in the flutter analysis. The finite element models included the main span portion of the overall bridge structure, which is defined by the locations at which the deck bending continuity with the approach spans is terminated. This arrangement resulted in analyzing the main span plus several shorter adjacent spans, as required for the particular configuration in question.

Figures 5 and 6 illustrate the steel and concrete finite element models. The outward appearances of the two models are alike except that the concrete model has one less pier and a slightly modified tower appearance. In reality, however, the deck properties obviously change as do the grid point locations and all mass and stiffness properties.

The deck geometry in the plan view is a straight line for somewhat less than half the span and a circular arc for the remaining part. The steel bridge initially analyzed is 1215 feet long and the concrete bridge is 1040 feet long. The deck describes a parabolic arc vertically with a peak elevation of 156 feet. The deck structure consists of the concrete slab of the roadbed and the integrally constructed concrete or steel supporting girders. The outermost girders are of fascia box construction. Figure 1C shows a typical cross section for the concrete alternate. The section properties change along the span as required by the design moments and the applicable design code loading conditions.

The tower supports the deck through pin supports. The four cable stays attach to the top of the tower and to the deck 175 feet on either side. The piers support the deck by roller type supports which permit relative longitudinal motions. The tower and pier footings are supported on pile groups which vary in size with 306 piles maximum for

the tower and 66 piles minimum for one of the piers.

The piling simulation is shown by Figure 7. Both pile elements and elements representing earth lateral stiffness are employed. Four simulated piles can provide a correct representation of pile group behavior, and this number was chosen to keep to a minimum the number of elements in the model. Each of the four piles in a simulated pile group consists of two BAR elements, and is fixed at the base (called the point of fixity) and provided with four springs (oriented parallel and perpendicular to the span) to resist motion relative to the surrounding earth. In the figure, for simplicity, earth springs are shown on only one pile. The point of fixity is determined from a detailed pile deflection analysis\*, and is the uppermost point at which zero pile bending slope occurs together with a very small pile deflection.

The earth spring element properties are defined by effectively integrating the distributed earth lateral stiffness over a pile length which is considered tributary to a particular pile grid point. The application of earth lateral resistance at only two points on the pile is an approximation of a type customarily made in discrete element analysis, and would not normally be a cause for concern. In the present case, however, because lateral earth stiffness was found to be a very important parameter, it was desired to verify the adequacy of the discrete representation. This was accomplished by comparing pile deflections computed for the two grid point pile to those obtained for a many grid point - many earth spring representation. The two grid point pile was found to predict deflection within 10% at the top of the pile. This accuracy is suitable for the dynamic analysis, and further refinement within the framework of linear elastic analysis does not appear worthwhile.

The simulated pile and earth spring stiffnesses in the finite element model are determined to provide the actual combined stiffness of the entire pile group. Denoting by  $k_h$  the earth spring stiffness which would be computed for one actual pile within a pile group, the following is the spring stiffnesses required in the finite element simulation.

$$k_{h \text{ model}} = k_h \cdot N \cdot \frac{1}{4}$$

$N$  is the number of piles in the group. The  $1/4$  factor distributes the total group earth lateral stiffness to the four simulated piles. In addition, the piles are located within the footing area (Figure 7) such that the moments of inertia of the simulated pile areas about the footing longitudinal and transverse axes match those of the actual pile group. This provides simulation of pile group bending stiffnesses. The use of  $N$  in the  $k_h$  formula would appear to presume that all piles in the group sustain equal lateral loads from the earth. Since this is known to be untrue, an adjustment was made in the  $k_h$  earth property to account for group pile action. The combination of group action and vibratory behavior in the earthquake was accounted for by taking  $k_h$  to be one-sixth the static, single pile value. This adjustment is based on reported research on group pile

\* Point of fixity and earth lateral stiffness data were provided by the firm of Shannon and Wilson, Soil Mechanics and Foundation Engineers, Seattle, Washington.

action<sup>(1)</sup>. However, in application to a particular pile group, such a factor is necessarily arbitrary, and it was felt necessary to evaluate the sensitivity of the structural behavior to variations in  $k_h$ . To accomplish this, a number of computer runs were made with widely varying earth spring stiffnesses. It was found that modal and earthquake response data are very sensitive to changes in earth spring stiffness for the case of relatively soft springs, with structural internal loads generally increasing with increasing spring stiffness. The final recommended spring stiffnesses are quite high, however, and in this range of values the modal and response data are reasonably insensitive to earth stiffness modifications.

The use of beam elements to represent the deck structure is an accurate idealization for all deformations except torsion. In the case of deck torsion, because of the torsion-bending behavior of the girders, a beam representation is necessarily approximate. The nature of the torsion-bending action is such that the effective torsional stiffness of the deck depends on the torsional mode shape, or wave length, to which the deck is subjected. This situation makes it possible to determine the deck torsional stiffness with acceptable accuracy by calculating the stiffness to correspond to the deck torsional vibration mode of greatest interest. The deck torsional modes are important principally because of their possible involvement in unstable aerodynamic motions (flutter). Therefore, the deck torsional stiffness was chosen specifically to obtain accurate modal data for the lowest (most flutter-critical) deck torsional mode. The half wave length (one lobe) of this mode (see Figure 1) is about 200 feet. Using this length, and postulating reasonable girder bending deformations in participation with deck torsional deflections, the girder torsion-bending contributions to the deck effective torsional stiffness were determined. These contributions are summed with the true torsional stiffness contribution, i.e., those of the slab and the closed box stiffness of the fascia girders, to obtain the total approximate deck torsional stiffness.

This procedure necessarily leaves higher deck torsional modes with less accurate (too low) torsional stiffnesses, and in general leaves overall bridge modes somewhat in error. These errors are negligible since, in the former case, only the lowest deck torsion mode was found to be a possible flutter candidate, and in the latter case the overall bridge modes are dominated by tower and deck bending and gross deck translational influences. It should be noted again that the torsion approximations were necessitated by the need for a simple, rapidly computed model. To completely resolve the deck torsion problem, as was done in the 3D model, would have sacrificed the utility of the stick model in the rapid turnaround design support activity. This was an unsatisfactory alternative. Moreover, calculations of the stick and 3D model modes confirmed the accuracy of the approach used.

#### Coding Details

The SAIL (Structural Analyzer Input Language) input language (Reference 2) was used in conjunction with NASTRAN bulk data in setting up the structural idealization. Details of the coding are described briefly below.

(1) This adjustment was provided by the firm of Shannon and Wilson.

1. **Geometry:** In using SAIL, the bridge geometry was programmed in the same form as it was provided by the design engineers. The grid point coordinates were coded in terms of "nose stations", the independent coordinate employed to measure distances along the deck centerline. The input was greatly simplified through the use of NASTRAN's multiple coordinate systems. Cylindrical coordinates were used for the portion of the bridge to the left of the tower in Figures 5 and 6, which is a circular arc in planview. The remaining straight segment of the bridge was input in the rectangular cartesian coordinate system. In the vertical plane, the deck describes a parabolic arc of the form

$$Z = 155.7 - \frac{(\text{Nose Sta} - 17070.)^2}{36666.67}$$

which was coded directly into the SAIL input deck. An important advantage of the SAIL input lies in the fact that variable gridpoint locations and variable numbers of elements are handled in so simple a fashion that generation of multiple idealizations is a minor task.

2. **Multiple Point Constraints:** MPC equations were found to be a convenient and powerful tool in representing the various connectivities encountered in the bridge structure. Structural idealizations using MPC equations are described briefly below.
  - (a) The cables are rigidly attached to the deck at offset nodes.
  - (b) The deck is attached to the tower structure in such a manner that all degrees of freedom except deck vertical bending rotation are required to be compatible. In addition, the deck elastic axis is offset (vertically above) its supporting cross member in the tower structure, because of the depths of the girders, the cross member, and the bearing fitting hardware.
  - (c) Similar to the tower attachment described above, the vertically offset deck attachment to the piers was enforced by MPC equations. In this case the connectivity between the longitudinal motions of the deck and the piers was in some designs pinned and in some designs represented by a roller support.
  - (d) All footings are connected to the upper ends of the piles by full fixity conditions enforced by MPC equations.
  - (e) In the complex (3D) deck idealization discussed later, MPC equations provided the connectivity between the girder webs and the deck slab representation.

The repetitive nature of MPC equations suggests their generation by a subroutine. This is discussed briefly under item 3., below.

3. **External Data Generators (EDG):**
  - (a) The external data generator is a feature within SAIL which provides a subroutine type of input generation capability. It is most conveniently used for multiple generations of large groups of similar elements and/or grid points. In the present problem, this situation occurs for the pile foundations. The pile group, including the footing, is a set of 25 elements,

29 grid points, plus multipoint and single point constraint conditions. All of these input data are prepared by the EDG, in the manner of a subroutine, needing only one set of coding for any number of foundation designs to be generated. The use of the EDG permits simple and rapid parameter studies on items such as stiffnesses, dimensions, etc., of the pile foundations.

- (b) The extensive use of multiple point constraints was simplified by creating EDG's specifically for the generation of MPC equations. This was done for both cylindrical and rectangular cartesian coordinate systems. The parameter set for the EDG consists of a list of the two or more nodes to be constrained. The EDG recovers the coordinates corresponding to these nodes and automatically calculates the constraint equations for a full six degree of freedom connectivity. This is particularly useful when cylindrical equations are employed and in parametric studies where grid point changes would otherwise require numerous, potentially erroneous, hand calculations. The EDG for the pile group generation, described above, calls the EDG for MPC equations as required to fix the piles to the footings.

#### Computation Details

The steel bridge idealization shown in Figure 5 was analyzed in 23 different configurations corresponding to various design changes and parameter studies. The basic model consisted of 199 grid points, 95 CBAR elements, and 80 CONROD elements. There were 166 MPC equations which in combination with boundary conditions and matrix reductions reduced the eigenproblem to 158th order. The runs averaged 6 minutes CPU time on the IBM 370 to extract the eigenvalues by Givens' Method and compute 70 modes. About one-third of the computer time was spent in applying the MPC equations. The basic concrete bridge idealization shown in Figure 6 was analyzed in 5 different configurations. The model consisted of 167 grid points, 84 CBAR elements, and 64 CONROD elements. There were 149 MPC equations which in combination with boundary conditions and matrix reductions reduced the eigenproblem to 143rd order. The runs averaged 5 minutes 48 seconds CPU time on the IBM 370 to extract the eigenvalues and compute 70 modes.



## THREE-D MODEL

### Purpose

Although the stick model was conceived to be acceptably accurate for both the seismic and flutter studies, a refined idealization, the 3D model, was set up for the concrete alternate to verify the stick model accuracy. The model was called 3D in reference to the idealization of the bridge deck by a slab element (represented as a beam) and individual girder web and flange elements. The beam type idealization of the tower, piers, footings, and piles is unchanged from the stick model. A computer plot of the structure is shown on Figure 3.

As discussed earlier, the weakness of the stick model lies in its simulation of deck torsional stiffness as that of a single member, while in reality the built-up deck resists torsion largely through girder bending. Therefore, the 3D model has as its purpose the accurate representation of girder bending participation in the overall deck deformations.

### Description of the Deck Model

Figure 8 shows schematically three types of behavior of a slab-girder deck. The first two apply to a bridge curved in planform, and the last applies for either straight or curved decks. All indicate that deck bending, either vertical or horizontal, will couple with torsion. The three cases are explained in the text of the figure. Basically, the coupling results from two facts: (1) in curved decks, torsion results in lower flange motion toward or away from the center of curvature, with a consequent tendency toward hoop stresses; (2) in horizontal bending of slab-girder configurations, the elastic shear forces are aligned with the shear center of the section (above the deck) while the inertia forces are aligned with the mass center. The tendency toward coupling of bending and torsion which is described by the figure will affect vibration modes by tending to make the mode shapes three-dimensional in character and difficult to identify as pure bending or torsional motions.

In order to represent these coupling tendencies in the finite element mode, it is necessary to meet several requirements:

1. Individual girder flanges must be represented in at least axial and horizontal bending properties.
2. Diaphragms, cross-bracing, and girder web lateral bending stiffness, all of which control lateral motion and therefore hoop forces in the flanges, must be modeled.
3. Flanges must be properly "driven" by the webs; therefore webs must be attached to the slab in such a way that continuity of displacement and rotation components is provided.
4. Structural masses should be properly located.

All of these requirements were met except the fourth. In the location of the masses, to simplify the computational problem, the deck mass properties were concentrated at the centerline of the slab. For the designs studied, however, the resulting error in mass

placement was very small.

Figure 9 shows the elements used in the 3D model. The deck slab is represented as a beam having axial, vertical and horizontal bending and shear, and torsional stiffnesses. The centerline of the slab is assigned the deformational freedoms of the deck structure, which are the six linear and rotational displacements. All deck motions are constrained to these six freedoms. The fascia box girders have a closed cell torsional stiffness. This stiffness was added to the torsional stiffness of the deck slab. Flanges are represented by beam elements which have axial and horizontal bending and shear stiffnesses. The handling of the webs presented difficult problems. It is known, and was further verified by calculations, that the NASTRAN plate elements with bending, shear and direct stress stiffnesses are of poor accuracy when used as web elements of girders, particularly for unsymmetrical cross sections. The erroneous behavior arises from the membrane stiffness of the plate. In order to avoid this difficulty, the girder webs were represented by combining shear-only plates with bending plates whose only stiffness is lateral bending. Because the latter plates cannot maintain the spacing between the flanges and the deck, posts are used at the ends of the elements. The axial-force stiffnesses (areas) of the girder webs are assigned to the deck slab and to the lower girder flanges such that: (1) the elastic axis of the composite deck in vertical bending is preserved; (2) the bending moment of inertia of the web of each girder about the composite deck elastic axis is preserved. These conditions provide accuracy in girder and deck bending and torsional behavior. Axial stretching stiffness of the total deck structure, an unimportant factor in the modal analysis, is approximated by these conditions.

## Coding Details

As with the stick model, the 3D model made use of both external data generators and multiple point constraints. The geometry was complicated by the banking of the bridge deck (superelevation). Again due to the repetitive nature of the input, SAIL was uniquely suited for data preparation. The principal coding problem is the generation of grid point and constraint data for the nine girders.

The deck centerline geometry and the variable superelevation were computed within the SAIL coding, using the equations and data provided by the designers. Using the computed centerline and superelevation geometrical data in the input parameter set, along with component structural data, the deck structure EDG was called. The EDG set up the upper girder web (and flange) grid points, the lower girder web (and flange) grid points, the girder flange and web elements, the MPC equations which serve to couple the girder elements to the six freedoms of the deck centerline, and in addition defined the freedoms to be reduced in the eigensolution. The MPC equations rigidly connect the upper girder web grid point freedoms to the six freedoms of the grid points on the deck slab centerline. The EDG is called once for each nose station at which a deck grid point is located, thus significantly reducing the magnitude of the coding task. This idealization in effect imposes deck cross-sectional bracing (diaphragms) at each deck grid point. This is a correct requirement since the designed diaphragms are located at approximately the same nose station spacing as are the deck grid points.

### Computational Details

The 3D concrete bridge model shown in Figure 3 was subjected to modal analysis. The finite element idealization consisted of 623 grid points, 242 CBAR elements, 280 CONROD elements, 207 CQUAD1 plates, and 207 CSHEAR webs. There were 1945 MPC equations which in combination with boundary conditions and matrix reductions reduced the eigenproblem to 149th order. A CPU run-time of 19 minutes and 20 seconds on the IBM 370 computer was required to extract the eigenvalues by Givens' Method and to compute 20 modes.

### SEISMIC AND FLUTTER ANALYSES

The seismic analysis was performed by the response spectrum method. The full details of this method are outside the scope of this paper. Portions of the overall methodology are described in Reference 3. The earthquake input data used are in the form of response spectra, and are specifically derived for the West Seattle site conditions.

The bridge response was determined in terms of its normal vibration modes. The response spectrum method provides maximum individual modal responses to the earthquake excitation. Modal summation is required over very few modes, for most earthquake analyses, and is done either as an absolute value sum or a root-square-sum, based on judgement and recommendations from past experience (Ref. 3)

The response spectrum method uses for input the modal analysis data, consisting of vibration mode period, generalized mass, and mode shape. In particular, modal response depends on the degree of coupling between the mode and the uniform vector field which describes the motions of the earthquake. This aspect of the seismic analysis requires the accessing and processing of very large amounts of structural and modal data. A new computer program, used as a NASTRAN post processor, was written to perform the work. This program obtains all needed data from the NASTRAN checkpoint/restart tape. The set of data read from the tape consists of files EQEX, GPDT, MGG, LAMA, PHIG, and OEF1. The complete modal and seismic analysis can be done in a single computer run, or the NASTRAN and seismic runs can be done separately. The seismic post processing program was found to be very convenient and provided a rapid analysis tool. Overnight turnaround on combined modal and seismic analyses was routinely obtained.

Flutter analysis was done for two types of flutter mechanisms: (1) single degree of freedom stall flutter; and (2) classical bending-torsion flutter. The calculations were done by existing Boeing flutter analysis programs, based on theoretical methods which are beyond the present scope. Aerodynamic data were obtained from wind tunnel tests on models of the various bridge deck sections, and modal data were obtained from the NASTRAN analyses. A subroutine within the seismic program was used to read the normal modes from the NASTRAN checkpoint/restart tape and to punch out on cards the required rotation and vertical translation displacements of the deck.

---

Data provided by the firm of Shannon and Wilson

## TYPICAL NUMERICAL RESULTS

### Seismic Analysis

Each modal analysis computer run provided complete modal data, including element internal loads, and also SC4020 plots of the mode shapes. Figures 10 and 11 are computer plots of the modes which were predicted to be the most important seismic motions of the West Seattle bridge. The plots shown are for the concrete alternate, but all configurations show essentially the same principal types of motions. The first is a lateral swaying and the second a combined longitudinal - vertical motion which is strongly influenced by the cables. The latter is the bridge fundamental mode. These modes are important seismically for two reasons: (1) their modal frequencies lie in a range of strong seismic input; (2) their mode shapes involve essentially unidirectional motions of the major bridge masses, thus obtaining strong coupling with the uniform seismic excitation.

Figures 12 and 13 show tower moments and shears which were computed for the initial steel and concrete designs. The moments and shears shown are those resisting a lateral swaying motion, and are caused primarily by modes of the type of Figure 11. The stresses for the concrete alternate are larger than those for the steel due mainly to the greater deck mass of the concrete design and the close proximity of the concrete modal period to a period of strong seismic excitation. These results proved excessively severe for strength design purposes.

As described earlier, the dynamic analysis was continued in support of trade studies for the development of a design configuration which is satisfactory for earthquake conditions. Figure 14 shows the results obtained for a set of seven designs which differ from one another primarily in tower configuration. All designs utilize a steel deck structure. From these results tower alternate A was chosen as the recommended configuration. The figure lists the modes and modal periods which are critical for both longitudinal and transverse earthquake excitations, and gives the resulting maximum tower bending moments. The curve shown in the lower right corner of the figure is the earthquake response spectrum used in the calculations.

As discussed earlier, a matter of concern was the effect of the approximation of the deck torsional stiffness on the accuracy of the stick model modes. It was for this reason that the 3D model was used to compute a more accurate set of modal data. Figures 15 and 16 show 3D model modes corresponding to the stick model modes of Figures 10 and 11. The agreement in mode shape is excellent. Figure 17 shows the lowest 3D model mode in which deck torsion is important. This mode shape justifies the manner of computation (the choice of wave length) of the stick model deck torsional stiffness which was described earlier. Figure 18 shows a comparison of stick model and 3D model modal data for the first ten modes for the concrete alternate. The frequencies are tabulated together with a brief description of the modal motions. Note that in several cases corresponding modes have changed order slightly, due to small changes in closely spaced frequencies. A careful study of all modal data has shown that in the

The defining of these configurations and the choice of tower alternate A were done by the firm of Knoerle, Bender, Stone, and Associates, Inc.

et of the first ten modes only the ninth stick model mode fails to agree closely with a corresponding 3D model mode. All other modes show good agreement in both mode shape and frequency.

#### Flutter Analysis

The flutter wind speeds were determined for the initial concrete and steel designs and for the current configuration which has been optimized for dynamic response conditions. For the initial concrete and steel designs, respectively, single degree of freedom stall flutter was predicted at steady horizontal windspeeds of 77 miles/hour in the lowest torsion mode and 46 miles per hour in the fundamental vertical bending mode. For the optimized design a torsion stall flutter speed of 244 miles per hour was predicted, with the improvement primarily a result of improved aerodynamic shape of the deck section and increased torsional stiffness of the closed box girder design.

#### CONCLUSION

The results of the dynamic analyses showed that the initial bridge designs were deficient in their ability to withstand a major earthquake or a sustained high wind condition. Through the early dynamic analysis parameter studies, however, the directions required for fruitful design modification were defined. A continuing program is in progress to implement these modifications into the design. This work has resulted in a bridge configuration which is satisfactory in resistance to both seismic and wind-induced motions. Currently, further design trade studies in conjunction with dynamic analysis are underway to optimize the design of the lower portion of the tower and the bridge foundation for improved earthquake resistance.

This use of the NASTRAN system in the field of civil engineering structures has demonstrated a potential for such applications. The benefits of such sophisticated analysis appear particularly great in consideration of the complex structural configurations and severe design conditions which are becoming increasingly common in the field of civil engineering structural design.

#### References

1. Jones, R.E., and Wagner, R.T.: Dynamic Analysis of the Proposed West Seattle Freeway Bridge. Boeing document D180-15357, 1973.
2. Ice, M.W.: NASTRAN User Interfaces - Automated Input Innovations. NASA TM X-2378 Colloquium, Langley Research Center, Hampton, Virginia. Sept. 1971.
3. Harris, C.M., and Crede, C.E.: "Shock and Vibration Handbook", Volume 3 McGraw-Hill, 1961, Chapter 50.

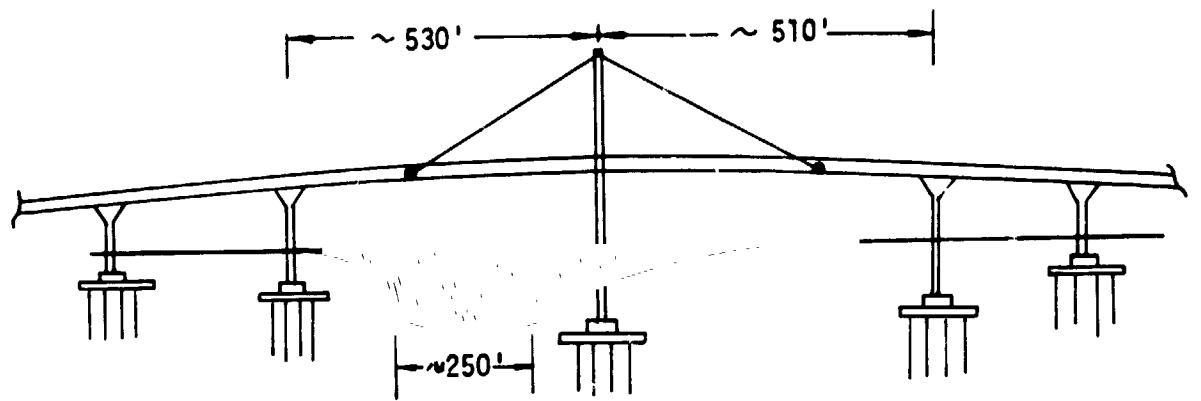


Figure 1a: ELEVATION VIEW

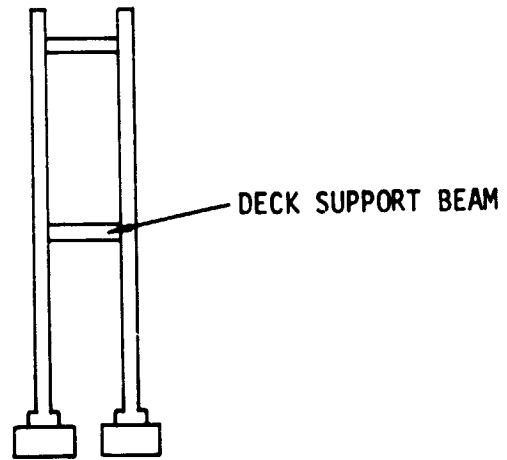


Figure 1b: TOWER CONFIGURATION- ELEVATION VIEW

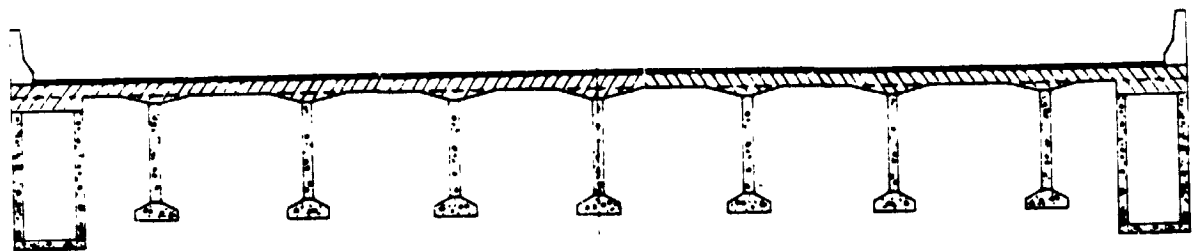


Figure 1c: TYPICAL DECK CROSS-SECTION

Figure 1: INITIAL BRIDGE DESIGN CONFIGURATION

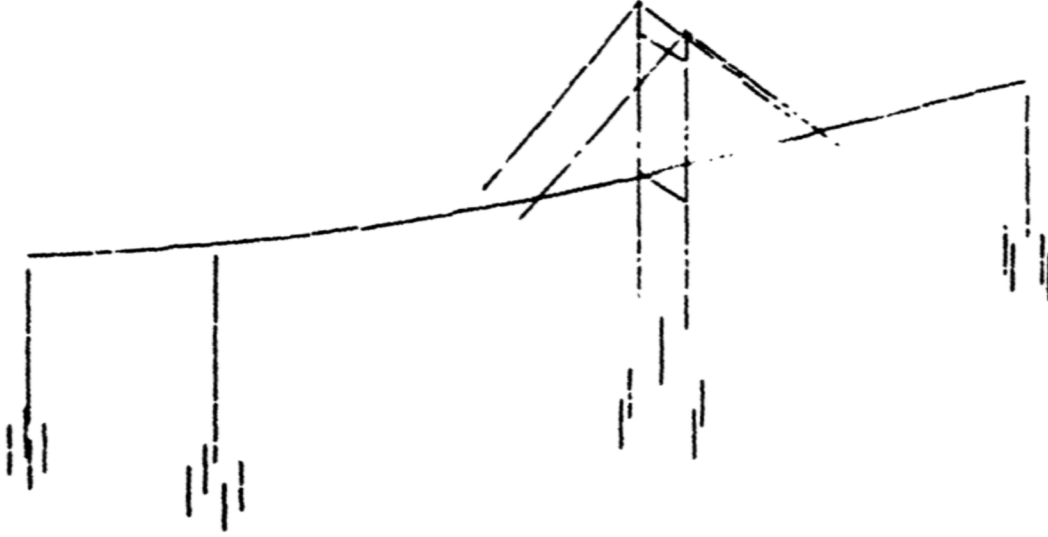


Figure 2: SIMPLE MODEL-CONCRETE ALTERNATE

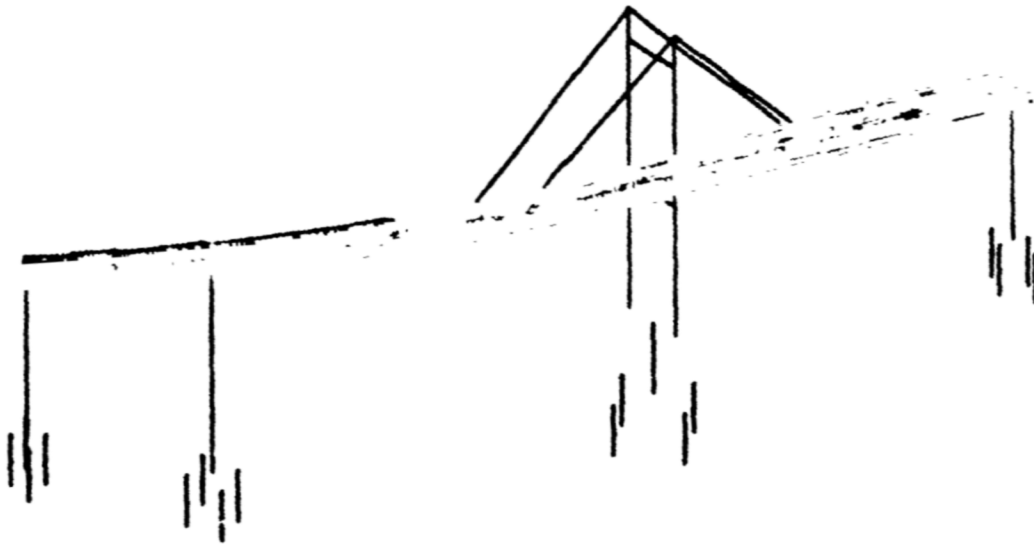


Figure 3 : THREE - D MODEL -- CONCRETE ALTERNATE

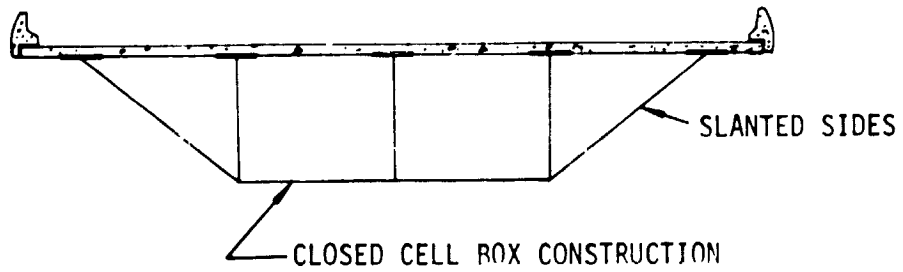


Figure 4a: DECK CROSS-SECTION

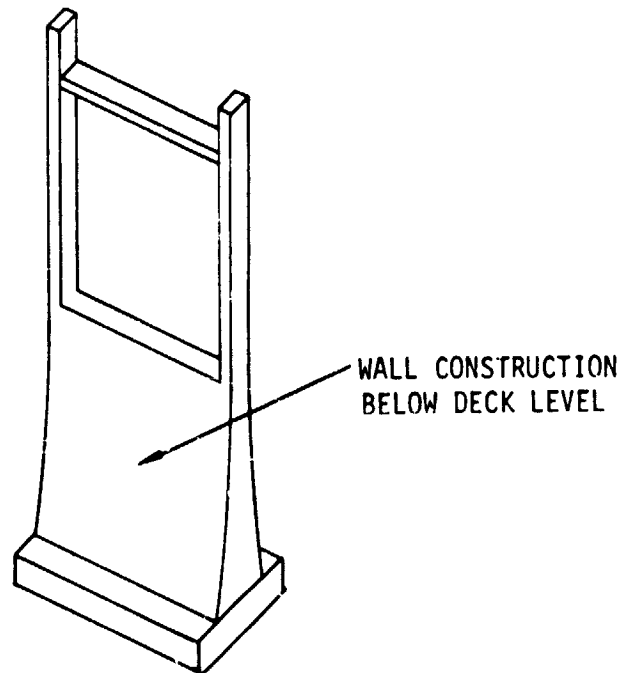


Figure 4b: TOWER CONFIGURATION

Figure 4: STRUCTURAL CONFIGURATIONS TO RESIST EARTHQUAKE AND HIGH WIND CONDITIONS



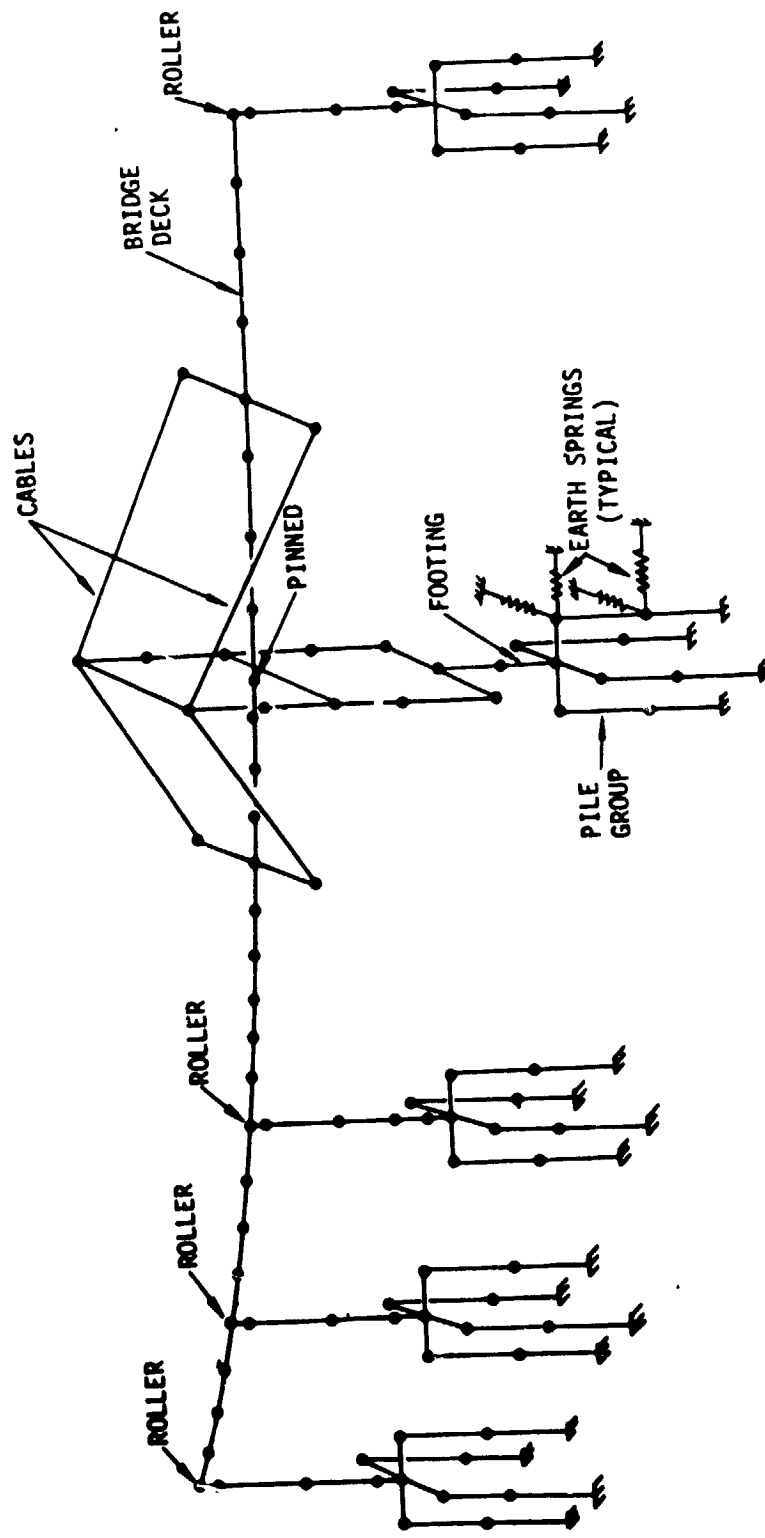


Figure 5 : STEEL FINITE ELEMENT (STICK) MODEL

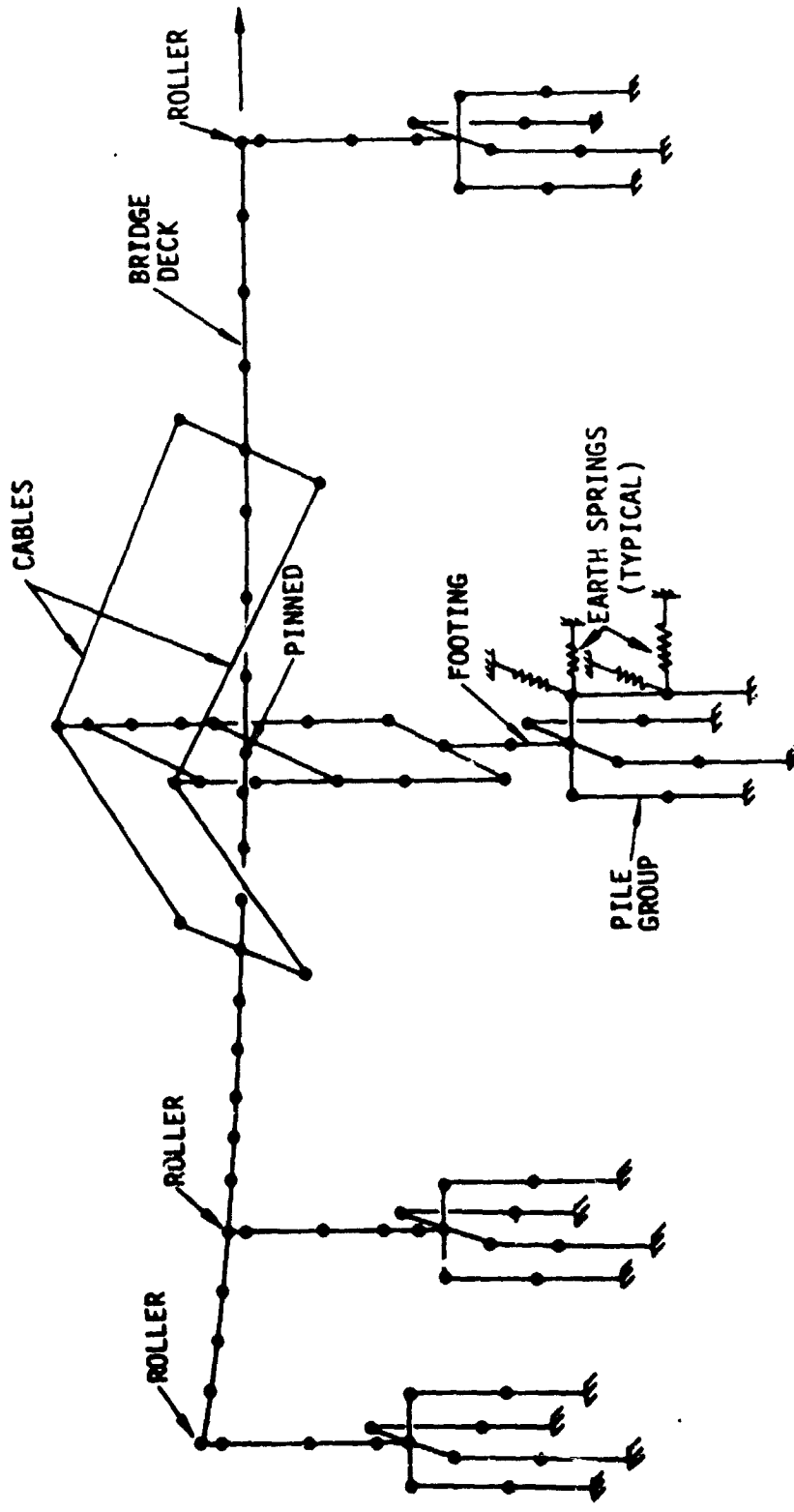


Figure 6 : CONCRETE FINITE ELEMENT (STICK) MODEL

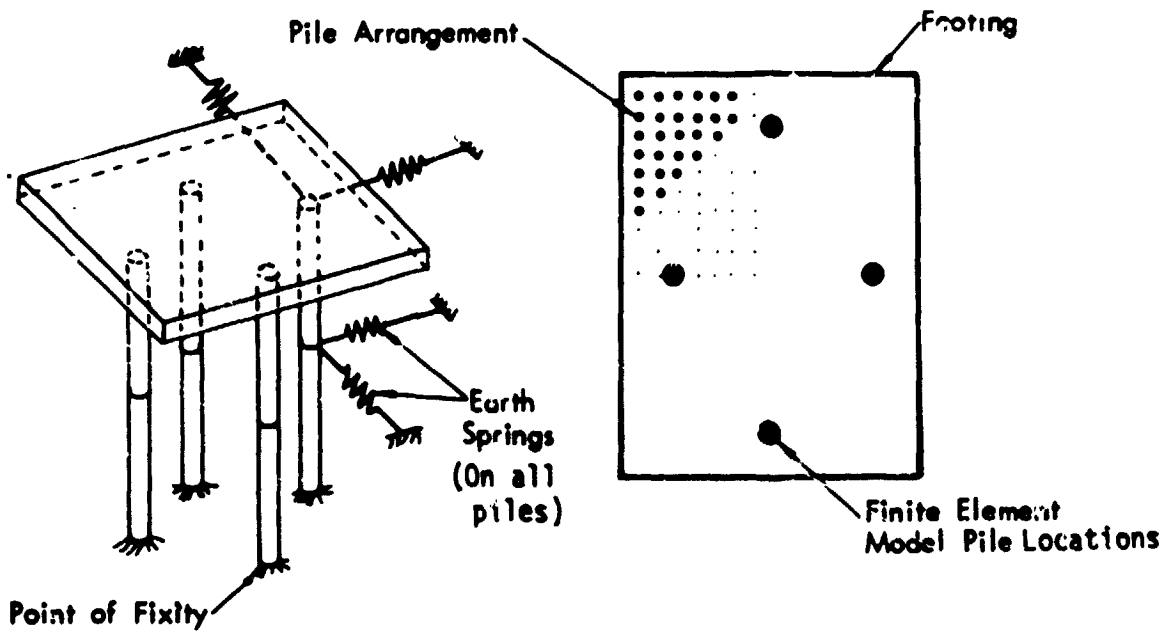
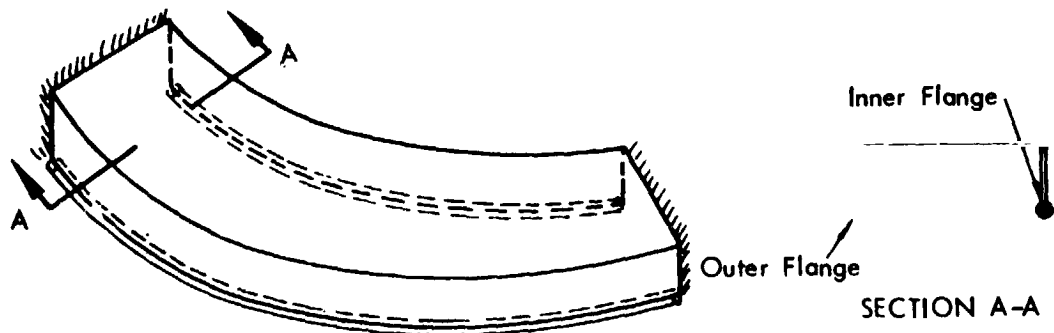
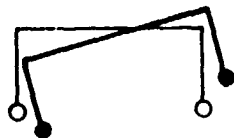


Figure 7 : FINITE ELEMENT PILE ARRANGEMENT



Basic Mode of Deformation

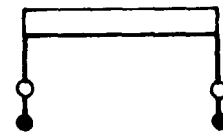


Lower Flange Compression

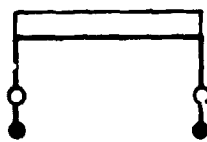
Torsional Deformation Causes Axial (Hoop) Stress in Flanges, Tending to Cause Vertical Bending Deformation For Stress Relief



Coupling Mode of Deformation



Downward Displacement

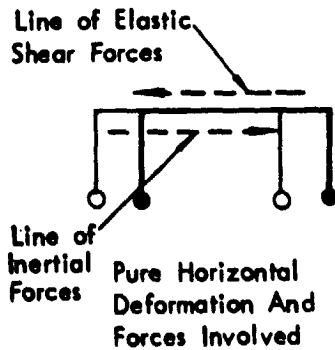


Lower Flange Tension

Vertical Displacement Causes Axial Stress in Flanges, Tending to Cause Horizontal and Torsional Deformation for Stress Relief



Horizontal and Torsional Displacement

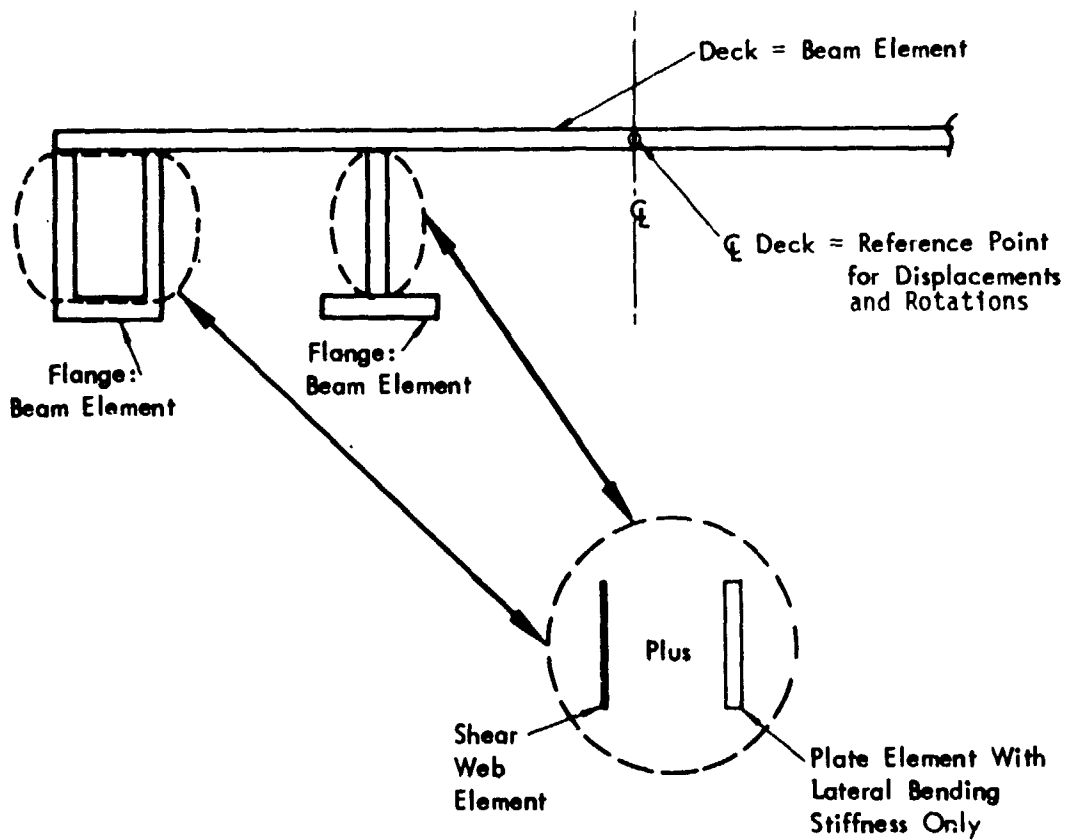


Horizontal Displacement Involves Horizontal Shear Forces of Elastic Behavior and Also Inertial (Mass) Behavior - Torsional and Horizontal Motions Tend to Couple



Coupled Torsional And Horizontal Motion

Figure 8 : BENDING-TORSION COUPLING OF SLAB - GIRDER DECK



- NOTES:
- o Girder Web Axial Area Assigned to Deck and Flange.
  - o Box Torsional Stiffness of Fascia Girder Assigned to Deck.
  - o Deck - Flange Spacing Maintained by Posts at Ends of Elements.

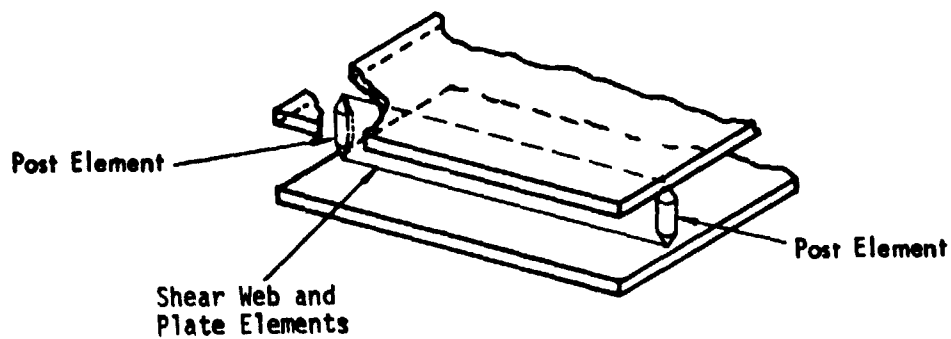


Figure 9 : ELEMENTS USED IN 3D MODEL

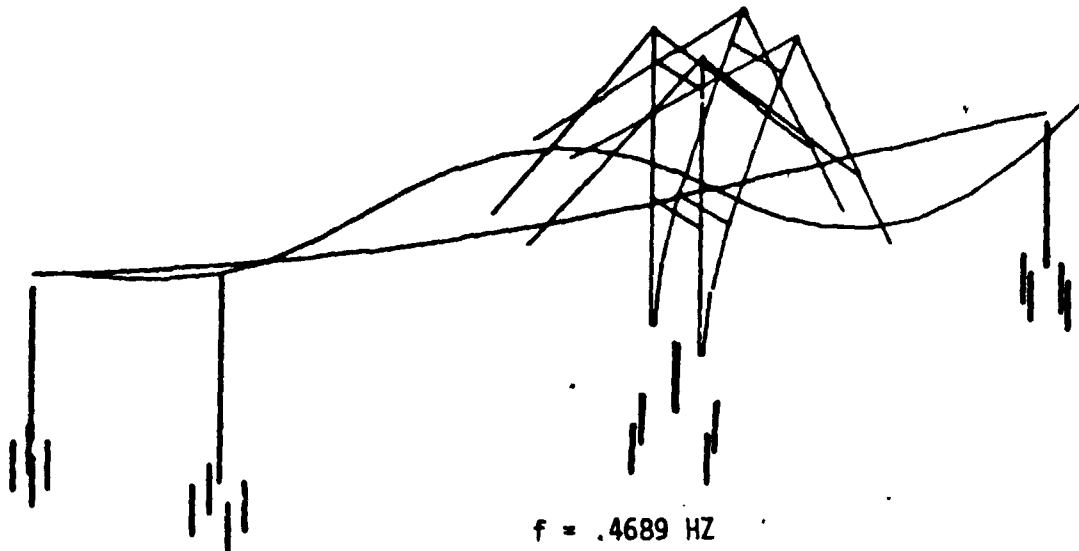


Figure 10: LONGITUDINAL AND VERTICAL MOTIONS  
- CONCRETE ALTERNATE

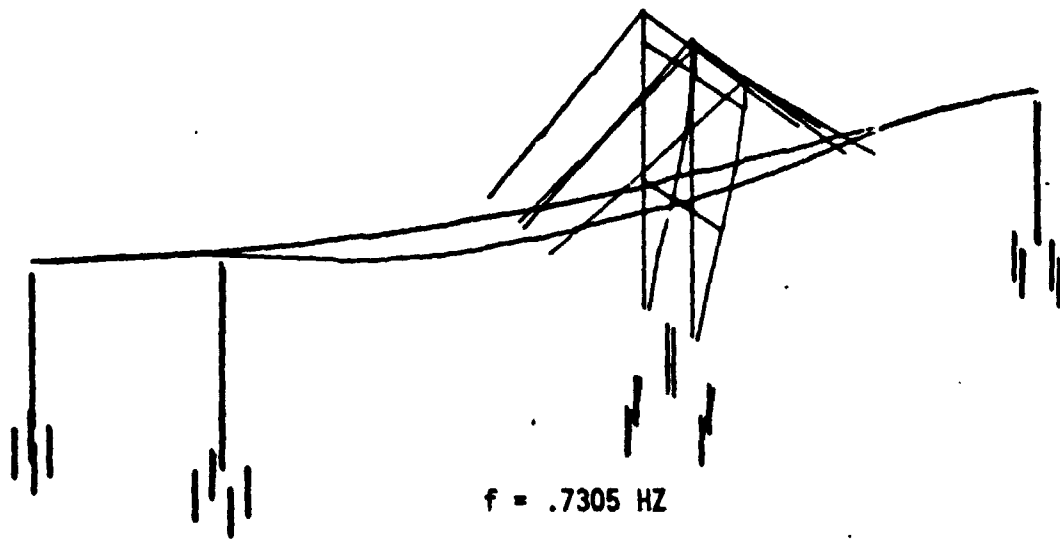


Figure 11: LATERAL MOTION- CONCRETE ALTERNATE

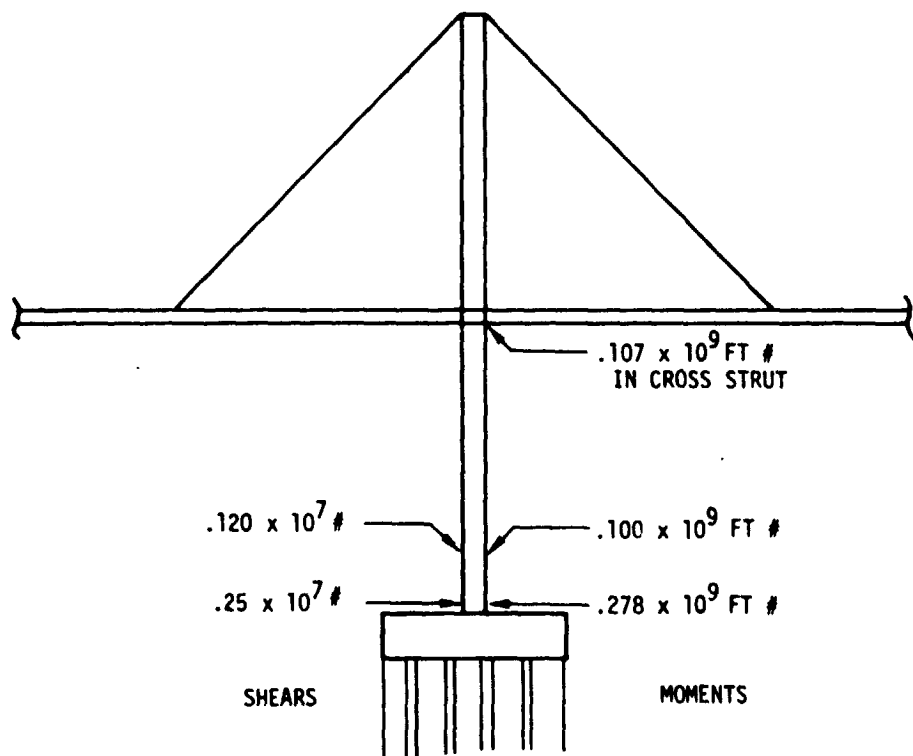


Figure 12 : SEISMIC MOMENTS AND SHEARS IN TOWER - STEEL ALTERNATE

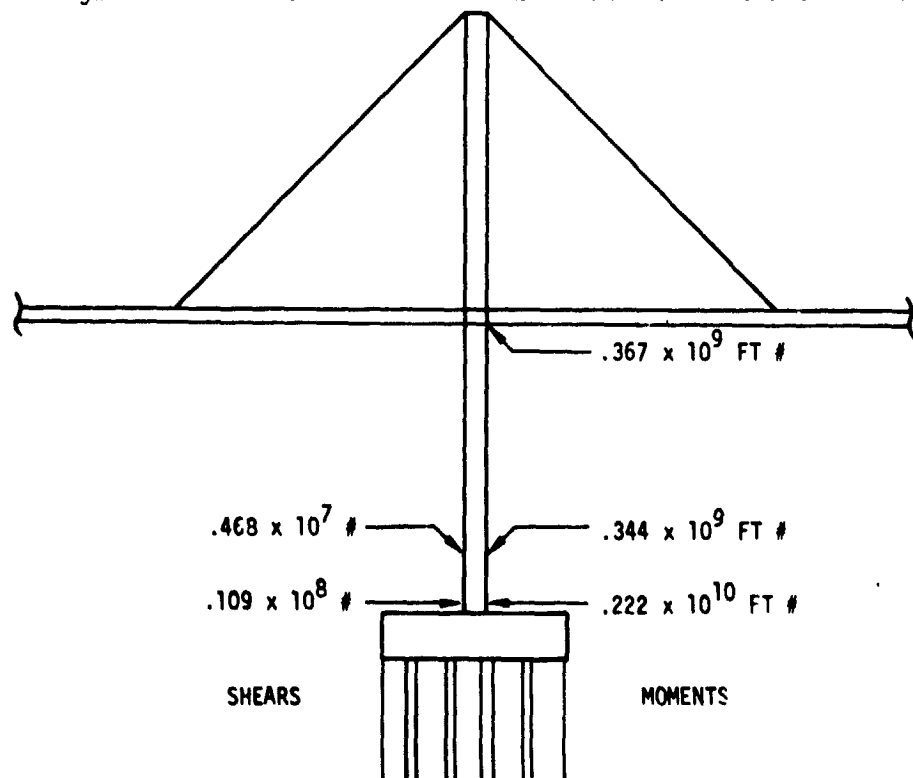
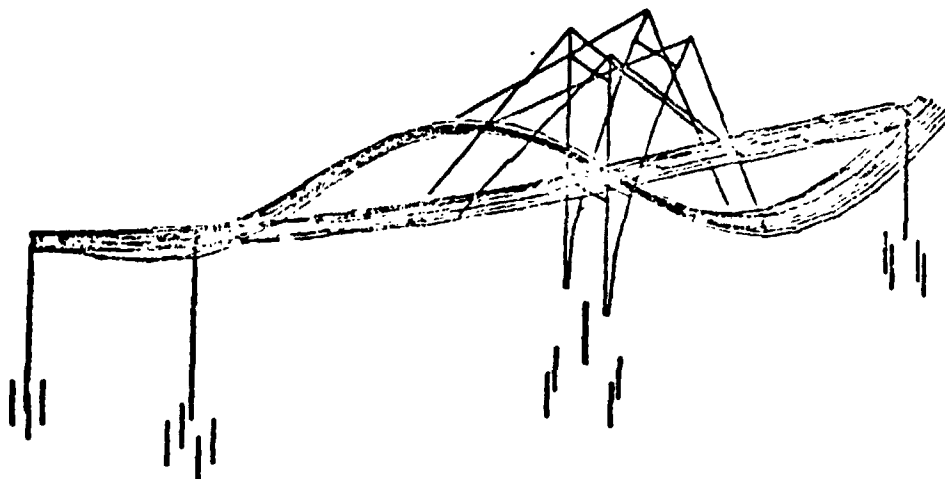


Figure 13 : SEISMIC MOMENTS AND SHEARS IN TOWER - CONCRETE ALTERNATE

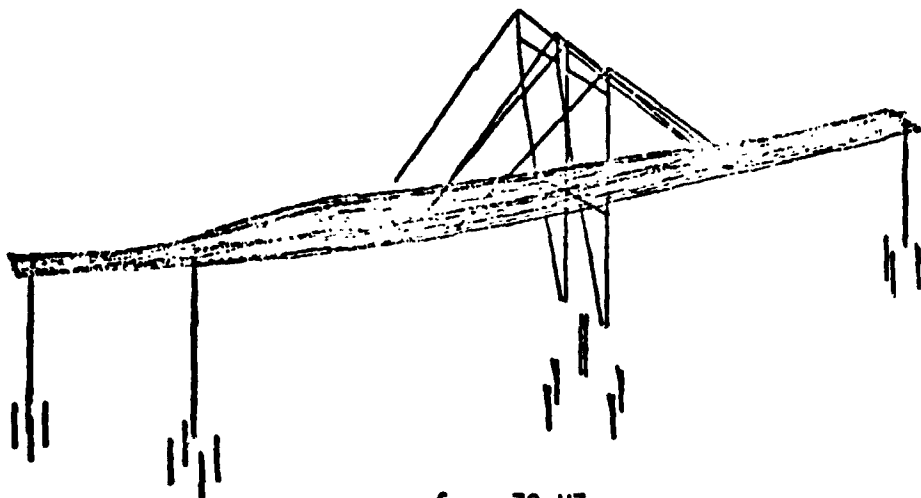






$f = .44 \text{ HZ}$

Figure 15: LONGITUDINAL AND VERTICAL MOTIONS -CONCRETE ALTERNATE



$f = .70 \text{ HZ}$

Figure 16: LATEKAL MOTION - CONCRETE ALTERNATE

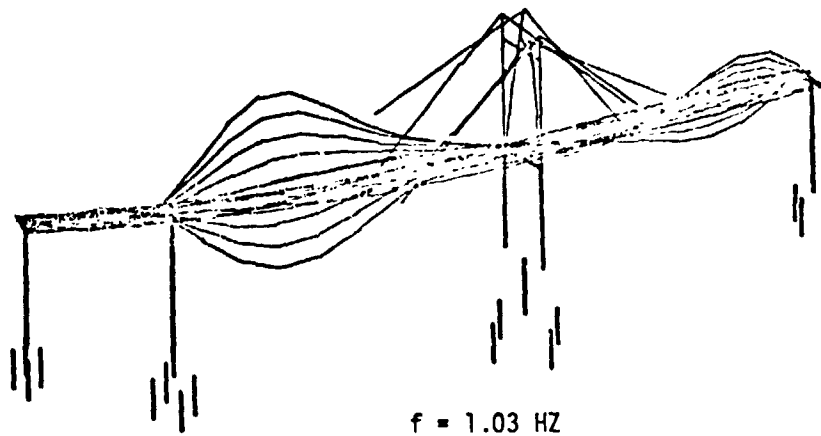


Figure 17: LONGITUDINAL, VERTICAL AND TORSION MOTIONS  
- CONCRETE ALTERNATE

CONCRETE ALTERNATE - STICK MODEL		CONCRETE ALTERNATE - 3D MODEL	
FREQUENCY (HZ)	MODE TYPE	FREQUENCY (HZ)	MODE TYPE
.4689	Y, Z	.44	Y, Z
.7132	Y, (P)	.70	X
.7305	X	.71	Y, (P)
.8109	Y, (P)	.81	Y, (P)
.8537	Y, Z	.81	Y, Z
.9429	Y, Z	.87	Y, Z
.9513	Y, (P)	.95	Y, (P)
1.014	Y, Z, T	1.03	Y, Z, T
1.065	X, Z, T	1.15	X, Y, Z, T
1.244	X, T	1.19	X, T

X = LATERAL  
 Y = LONGITUDINAL  
 Z = VERTICAL  
 T = TORSION  
 (P) = PIER ONLY

Figure 18: COMPARISON OF 3D AND STICK MODEL MODAL DATA